ASME Turbo Expo 2020: Turbomachinery Technical Conference and Exposition,
September 21–25, 2020, Virtual Event, GT2020-15329
DOI:https://doi.org/10.1115/GT2020-15329

APPLICATION OF MODEL BASED SYSTEMS ENGINEERING FOR THE CONCEPTUAL DESIGN OF A HYBRID-ELECTRIC ATR 42-500: FROM SYSTEM ARCHITECTING TO SYSTEM SIMULATION.

Federico Cappuzzo[1], Olivier Broca[1], Stavros Vouros[2], Ioannis Roumeliotis[2], Calum Scullion[2]
[1]Siemens Digital Industries Software, Lyon, France
[2]Cranfield University, Cranfield, UK

ABSTRACT

The progress in aerospace technology over the recent years led to the development of more sophisticated and integrated systems. To cope with this complexity, the aerospace industry is seeing a progressive trend towards adopting Model-Based Systems Engineering (MBSE) in various stages of the product development cycle. The ability to capture emerging behavior, mitigation of risk and improved communication among different stakeholders are some key benefits that MBSE provides over traditional methods for complex systems and processes. This paper attempts to bridge the gap between system architecting and system simulation activities by proposing a methodology to facilitate seamless flow of information between the two development aspects. This methodology was applied to the development of a parallel hybrid-electric version of the ATR 42-500. The use case was designed for a regional mission of 400 nautical miles with the ability to meet regulation requirement of carrying enough reserves for landing at an alternate airport. An integrated systems model, consisting of gas turbine engine, electric powertrain, and flight dynamics, was developed with Simcenter Amesim to analyze the dynamics performance of the aircraft throughout the whole mission. The key metrics evaluated were fuel consumption, take-off weight and the Energy Specific Air Range (ESAR) of the aircraft. As environmental regulations are becoming more stringent, pollutant and noise emissions were considered in the study. The most promising hybrid configurations are recognized, the potential benefits are quantified highlighting the strong potential of System Architecting and System Simulation to provide valuable insights early in the development cycle, reducing the time and cost of product development.

Keywords: MBSE, System Architecture, System Simulation, Hybrid Aircraft, Aircraft performance, Simcenter Amesim.

NOMENCLATURE

ACARE	Advisory Council for Aeronautics Research in Europe
E	Energy
EINOx	Nitrogen Oxides Emission Index
ESAR	Energy Specific Air Range
FCOM	Flight Crew Operating Manual
FOCA	Federal Office of Civil Aviation of Switzerland
L/D	Instantaneous Lift-to-Drag ratio
LP	Low Pressure
HP	High Pressure
H_P	Degree of hybridization
MBSE	Model Based Systems Engineering
M&S	Modelling and Simulation
MTOW	Maximum Take-Off Weight
OASPL	Overall Sound Pressure Level
OEW	Operating Empty Weight
P_{MCT}	engine power at maximum continuous thrust
R	Range
ROCD	Rate of Climb/Descent
SEL	Sound Exposure Levels
TAS	True Air Speed
TOW	Take-Off Weight
TSPC	Thrust Specific Power Consumption
VIA	Virtual Integrated Aircraft
W	Instantaneous aircraft weight

INTRODUCTION

With increasing prominence of air travel, there has been a tremendous progress in the technology of aerospace systems. As aircraft and their associated systems are becoming more sophisticated and integrated, the complexity of their development process is also increasing. This is due to a variety of factors like the large number of involved components, huge number of people and teams involved, stricter regulatory requirements on environment and safety, etc. [1][2]

In the recent years, aerospace industry is moving towards the next step in system engineering, i.e. Model Based Systems Engineering (MBSE), which involves the use of models to represent all the information regarding the system. The ability to capture emerging behavior, mitigation of risk and improved communication among teams are some of the key benefits that MBSE provides over traditional methods while modelling complex systems and processes as discussed by Hart [5]. Complexity is managed through the creation of what are known as architectures in MBSE, i.e. the formalization of the relationships between the system's forms (or entity) and functions (or activity) through descriptive models as extensively discussed in [3] and [4]. As discussed by Hart [5] MBSE supports the full realization of the potential of an integrated and collaborative environment in which a single source of truth act as the core model across the different stages of the product lifecycle.

It is common for the aircraft systems integration to take place during the final test and validation phase by physical prototyping. Any problems detected at this stage lead to huge cost and time overruns. The cost of corrective actions at testing stage is significant higher compared to the cost when any action is undertaken at design or build stage as discussed by Baskin et al. [6]. A solution to this problem is the Virtual Integrated Aircraft (VIA), a methodology relying on MBSE principles proposed by Siemens [7]. VIA enables the virtual integration of complex systems during the early stages of aircraft design process. Hence, achieving aircraft systems integration earlier in the development phase will be beneficial reducing the cost of modifications and the cost of expensive physical prototyping.

VIA methodologies rely on early stage Modelling and Simulation (M&S) techniques. Currently, the simulation models are developed either with the domain experience of the simulation engineer or pre-existing model data. But with the emergence of MBSE, there is a potential way to help the simulation engineer with inputs coming from the system architecture domain. This will ensure traceability of decisions and coherency of all the specifications. The models in system architecture capture several top level and system level requirements which can be translated to simulation domain with the use of MBSE. The results from simulation can then help drive architectural decisions in the system architecture domain. Hence, there is a need to transition from system architecture to system simulation in a logical manner. This paper attempts to bridge the gap between the two domains by using MBSE tools and methodologies. Air transport contributes about 3% of world greenhouse gas emissions [8]. Aircraft traffic is expected to grow at 4.3% annually over the next 20 years [8]. Extrapolating this trend, the passenger volume is expected to triple by the year 2050. For tackling the environmental challenge that this increase in traffic will pose for the aviation industry the Advisory Council for Aeronautics Research in Europe (ACARE) has formulated guidelines for "Flightpath 2050" setting a target of 75% cut in CO_2, 90% cut in NO_x and 65% reduction in noise for the aviation industry in 2050 [9]. Hybrid-electric concepts are proposed to address this challenge, hence the usage of electric power for aircraft propulsion has become a compelling business case [10]. Additionally, hybrid electric propulsion configurations integrate systems from different physical domains allowing the assessment of the method, highlighting the critical aspects and the potential benefits.

For these reasons, the conceptual design of a parallel hybrid-electric configuration was selected as a use-case. Recent research showed how hybrid propulsion is particularly suited for small regional transport aircraft concept (~50 passengers), as it can deliver significant cost and performance advantages over current aircraft of the same class in a reasonable short timeframe [11]. In this context the hybridization of ATR 42-500 twin-turboprop, short-haul regional airliner is analyzed herein utilizing the VIA methodology.

USE-CASE DESCRIPTION

The use-case chosen for the project is a regional hybrid aircraft with an entry into service planned for 2030. One of the top-level aircraft requirements to provide for the case study is the aircraft range, which indicates the maximum distance it can travel at a given take-off weight. It is predicted that in 2030 about 90% of regional trips will be less than 400 nautical miles as discussed by Marien [12]. The distribution of trips with respect to distance expected for 2030 is shown in ***Figure 1***. For this reason, an operative range of 400 nmi was selected for the study. This range is typical of turboprops regional aircraft with a seating capacity of around 50 passengers [13].

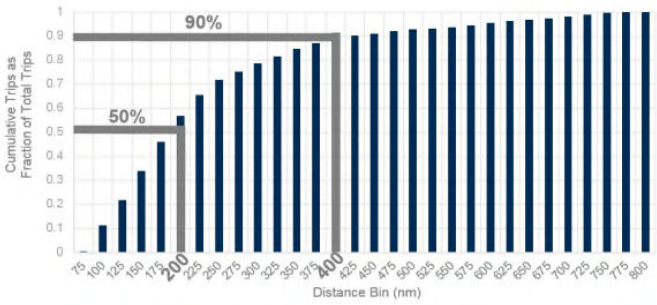

Figure 1: Cumulative distribution of trips with respect to distance predicted for 2030 [12].

According to these two drivers (operative range and passenger capacity), the current study selected the ATR 42-500 as a promising candidate for a conceptual parallel hybrid version, as presented in a study by NASA Langley Research Centre [10]. ATR 42-500 is a popular under-50 seat plane in regional aviation. The first model of ATR 42 had its maiden flight in 1984. It is a single-aisle aircraft equipped with 2 turbo-prop engines (PW 127) as shown in **Figure *2*.**

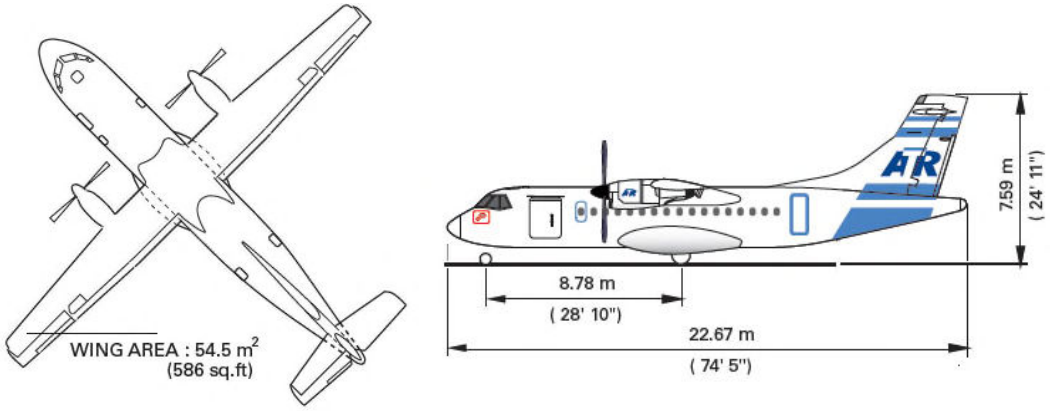

Figure 2: Top view and side view sketches of ATR 42-500 [14].

The regulation given by European Union Aviation Safety Agency (EASA) [14] requires that the aircraft must carry additional fuel called "reserve fuel" which should be enough to fly to an alternate destination airport and fly for an additional 45 minutes at cruise speed. For an ATR 42-500, the alternate destination airport distance used for the published performance is 87 nautical miles. The distance travelled during 45 minutes of cruise flight is almost equal to 225 nmi at a cruise speed of 300 knots. The developed hybrid aircraft will have to carry enough reserves to fly 300 nmi in addition to the trip distance. This constraint may be relaxed in 2030 as it is a very demanding requirement for a hybrid aircraft, but it is nevertheless considered for this study to follow a conservative approach. An example of "reserve mission" is depicted in ***Figure 3***, and it was reconstructed using the ATR 42-500 FCOM for a TOW of 19t. It is composed of two parts: the nominal part, with a target range of 400nmi at an altitude of 18000ft, plus the reserve part. The latter is comprehensive of a climb to cruise level, a cruise flight to cover (together with the climb) 87nmi to reach the alternate airport, a 45 minutes flight at cruise speed as required by regulations, and landing. The transition between the two parts was chosen to be arbitrarily at an altitude of 8000 ft during descent.

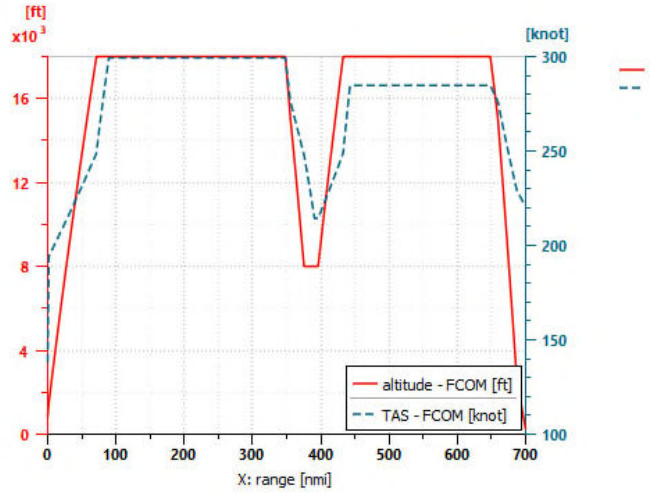

Figure 3: ATR 42-500 reserve mission, TOW 19t. Altitude and TAS plotted versus the travelled distance.

An important requirement to consider for the conceptual design of a hybrid electric aircraft is the battery specific energy, i.e. the amount of energy stored per unit mass of the battery. This is a critical factor in hybrid aircraft design for its contribution to determine the overall mass of the aircraft. State-of-the-art batteries have a specific energy of about 250 Wh/kg [17]. A study conducted by Brelje and Martins [16] on the historic and upcoming hybrid aircraft concepts compiled the data regarding their battery specific energy. By interpolating the data, a value of 750 Wh/kg was obtained for the year 2030 as shown in **Figure *4***. Another study by Kuhn and Sizmann [17] addresses the prospects for future lithium battery technology for fully-electric air transport. The authors argue that lithium-air and lithium-sulfur batteries are expected to reach an energy density of 600 Wh/kg or higher. Based this data, an average value of 650 Wh/kg was selected for this study. The payload and the maximum cruising speed reflect those of the conventional version ATR 42-500 as reported in [15], with the intent of providing the same operational performance.

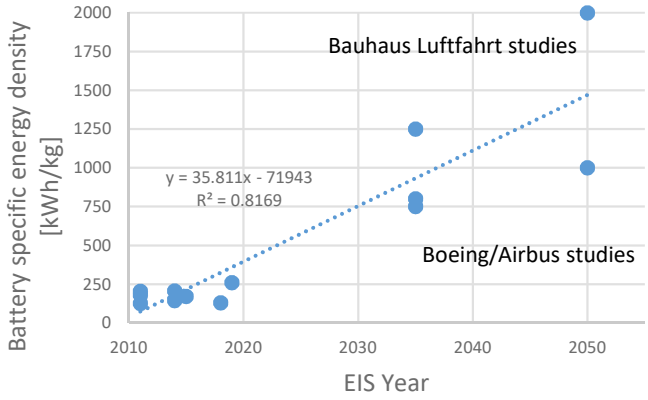

Figure 4: Battery specific energy data of previous, existing and upcoming hybrid aircraft concepts [16] (added trendline).

The top-level aircraft requirements considered for this analysis are summarized in **Table *1***.

Table 1: Top-level aircraft requirements.

Top-level aircraft requirements	
Payload	5300 kg (48 pax)
Max. cruise speed	0.5 Mach
Battery specific energy	650 Wh/kg
Range	400 nmi
Constraint of meeting alternate airport and reserve fuel regulation	Additional distance - 300 nmi (approx.)

A hybrid variant of this aircraft consists in retrofitting its gas turbine engines with turbine-electric motors in a parallel configuration, where the propeller is driven simultaneously by the electric motor and the gas turbine as shown in ***Figure 5***. This paper investigated this configuration at different degrees of hybridization (Hp), defined as the ratio of maximum electric power installed in the aircraft to the maximum power capacity of the complete powerplant. Hp values of 20%, 40%, and 60% were evaluated.

$$H_P = \frac{P_{EM,max}}{P_{max}} \quad (1)$$

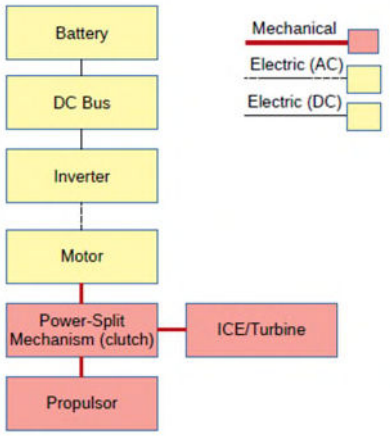

Figure 5: Parallel-hybrid propulsion configuration [16].

To evaluate the hybrid-aircraft performance, the following metrics were selected:

1. **Energy Specific Air Range (ESAR)**, expressed in m/MJ, provides the amount of distance traveled (R) per unit of energy consumed (E) [19]

$$ESAR = \frac{dR}{dE} = \frac{V_{TAS}\,(L/D)}{TSPC \cdot W} = \frac{\eta_{ov}(L/D)}{W} \quad (2)$$

Where:

- V_{TAS} is the true airspeed in m/s
- L/D is the instantaneous Lift-to-Drag ratio
- $TSPC$ is the Thrust Specific Power Consumption, expressed in W/N, which accounts for the power provided by both batteries and fuel
- W is the aircraft weight, in N

- η_{ov} is the overall efficiency of the motive power system

2. **Block Fuel consumption**, expressed in kg, directly impacts the aircraft emissions and cost of operations. Since the regulation requires the aircraft to carry enough fuel for the reserve mission as well, both the 'mission fuel' used for the trip and 'reserve fuel' used for the safety scenario are important to evaluate.

3. **Take-Off Weight (TOW)**, in kg, composed of the Operating Empty Weight (OEW), plus the mission and reserve fuel and the weight of electric motors and batteries. TOW greatly affects the aircraft performance.

4. **Pollutants emissions** in kg, specifically CO_2, H_2O and NO_x are assessed. CO_2 and H_2O as products of combustion are directly calculated from Simcenter Amesim from the total fuel consumption (m_f) and the ratio of the molar mass of CO_2, H_2O and kerosene ($C_{10}H_{20}$) assuming a stoichiometric equilibrium:

$$CO_2(kg) = m_f \cdot 10 \frac{M_{CO_2}}{M_{C_{10}H_{20}}} \quad (3)$$

$$H_2O(kg) = m_f \cdot 10 \frac{M_{H_2O}}{M_{C_{10}H_{20}}} \quad (4)$$

NOx emissions are calculated using the FOCA correlation with shaft horse power (SHP) [20].

$$EINOx\left(\frac{g}{kgf}\right) = 0.2113 \cdot SHP^{0.5677} \quad (5)$$

Additionally, it should be considered that the batteries are fully charged at the start of the mission, while they are discharged to some extend at the end of the mission. For accounting the emissions due to recharging the batteries at the end of the mission from the grid a value of 0.42 $kgCO_2/kWh$ is applied according to [21].

5. **Acoustic footprint**, expressed as Sound Exposure Levels (SEL), which includes both the sound levels and duration of exposure.

$$SEL(dB) = 10 \log_{10}\left[\int_{t_1}^{t_2} 10 \frac{OASPL(t)}{10} dt\right] \quad (6)$$

FROM SYSTEM ARCHITECTING TO SYSTEM SIMULATION

System architecting is an integral part of the systems engineering activities and forms the core of different product lifecycle activities. System architecting can be explained as the process of finding the best solution which meets the given requirements and constraints. It involves formalizing the system in different views to explain its various aspects. As part of MBSE, system architecting involves capturing the operational, functional and non-functional behavior of a system in the form of models. There can be multiple diagrams representing the same underlying model of the system. Using models allows obtaining the right level of abstraction or refinement required for a given activity. For example, to model the high-level behavior of a system, it is only required to understand the system-level functions without going too much in-depth about the sub-systems. On the other hand, to understand the various physical and component exchanges inside a system, it is required to go to lower levels of architecture like logical or physical. MBSE allows this flexibility of shifting between architecture viewpoints
and since all of them are connected, changes made at any architecture stage are reflected in others. The methodology chosen for this project was ARCADIA [22], embedded in the Capella tool [23]. The four main steps prescribed by the methodology are the operational analysis, system analysis, logical analysis, and physical analysis. The first two stages deal with understanding the needs and requirements of various stakeholders while the latter two provide architectural solutions satisfying the identified needs. The basic philosophy of the methodology is a top-down approach in which architectural decisions at each stage are taken in order to satisfy some need or refine the architecture developed in the preceding stage. This ensures continuity and justification of the workflow and each engineering decision is traceable. The overall methodology of transitioning from system architecting to system simulation involved three different software tools as shown in ***Figure 6***.

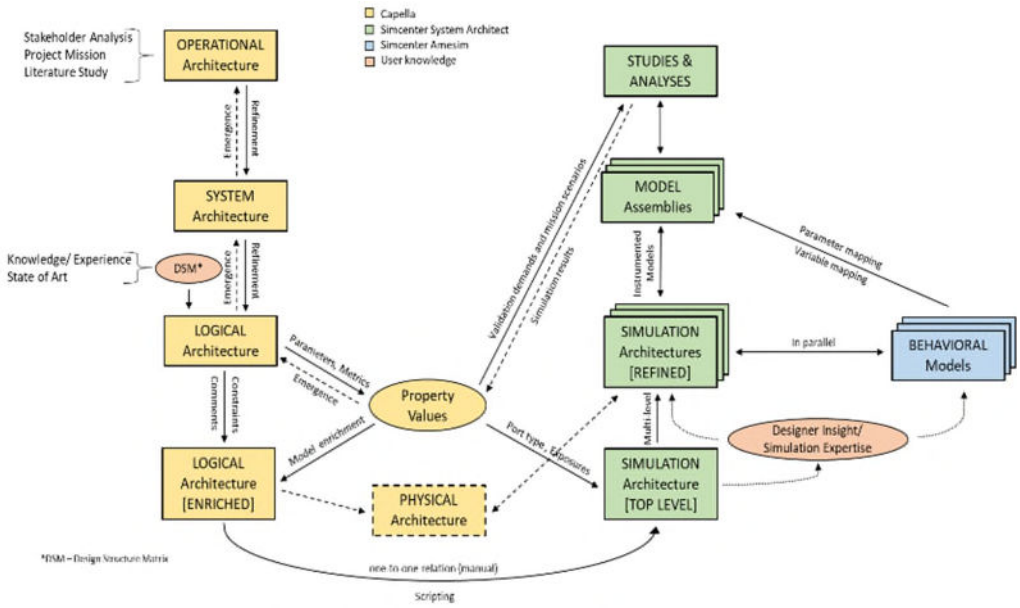

Figure 6: Methodology of transitioning from system architecture to system simulation.

Initially, the operational architecture of the system was modelled, driven by the stakeholder-needs and top-level aircraft requirements summarized in Table 1. This was refined into a system architecture by translating operational needs to system-level requirements. Now, a first trade-off study was performed dividing the system into different sub-systems to obtain the logical architecture, enhanced by embedding additional model information through property values management tool. The enriched logical architecture in Capella contained enough information about the hybrid-aircraft system to start developing the simulation architecture.

The components of the logical system were defined in Simcenter System Architect as "base templates" using a one-to-one mapping. To create "simulation templates" in System Architect, the information contained in the property value of Capella was utilized. After assembling all the simulation templates in the same fashion as logical architecture, a full simulation architecture (top-level) was obtained. The next step after obtaining a top-level simulation architecture is developing refined versions of the simulation architecture. This process is done in parallel with modelling the behavioral models in an authoring tool like Amesim. As the components of the hybrid aircraft were known from state of the art, all the components required for simulating the performance of the hybrid-aircraft like gas turbine, propeller, aircraft body, etc. were modelled in Amesim. Corresponding to this model, another team in the company developed a simulation architecture (refined) in System Architect. The two simulation architectures – top level and refined were compared to identify the similarities and differences between the two. Later, an iterative process was followed to develop the different Amesim models corresponding to the hybrid-aircraft use-case. The behavioral models from Amesim were then imported in System Architect to map the corresponding components between the two tools. These models with mapped ports and variables are called instrumented models.

The instrumented models were then assembled to form the complete hybrid-aircraft system which was simulated in multiple conditions to obtain different results. Finally, these results were used to make trade-off studies for identifying the best architectural solution. This information can then be fed back to the system architecting domain through property values tool and back-tracing. This would allow the logical architecture to consist of an architectural solution validated by simulation. Hence, the subsequent stages of ARCADIA process like physical architecture could then be developed using information from logical architecture as well as simulation architecture. The simulation results could also be analyzed to observe and propagate the emergent behavior of the integrated system to different system architecting levels.

MODELING AND SIMULATION

The first step of the modeling activities consists of developing a system simulation model of the conventional version of the ATR with Simcenter Amesim [24], a dynamic multi-physics system simulation tool. This will provide means to validate the model against the data available, validating in turn the modelling assumptions and the tools used. Given that

there was more data available in the literature for the ATR 72-600 [25][26][27] compared to ATR 42-500 [28], it was decided first to model the ATR 72-600 aircraft, validate the modeling strategy, and then derive the ATR 42-500 model down-scaling the engine and modifying the aerodynamics coefficient to account for the different geometry. The validated conventional model will serve as a baseline to compare the performance evolution of the different levels of hybridization.

Then, the hybrid aircraft models are created. The reserve mission scenario is simulated, and the overall mission performance assessed. Finally, the simulation results obtained were then fed to the code ICARUS [29] of the Cranfield University to run the aeroacoustics analysis.

ATR 72-600 modeling and validation

Given the larger amount of public available data, the ATR 72-600 aircraft was developed to validate the modeling strategy, and then derive the ATR 42-500 model. The aircraft performance model, created with Simcenter Amesim, is shown in ***Figure 7***. For the aircraft performance analysis, the point mass assumption was considered adequate for the flight dynamics modeling [30]. From ***Figure 7***, it can be noticed that only half of the powerplant was modeled with the purpose to reduce the model's complexity and obtain CPU times of around 15s for a complete mission of 70 minutes (run on a regular laptop). This was possible thanks to the symmetricity of the powerplant and to the fact that no scenarios concerning uneven thrust were required to be analyzed. Looking at the picture from right to left, the model consists of the following components:

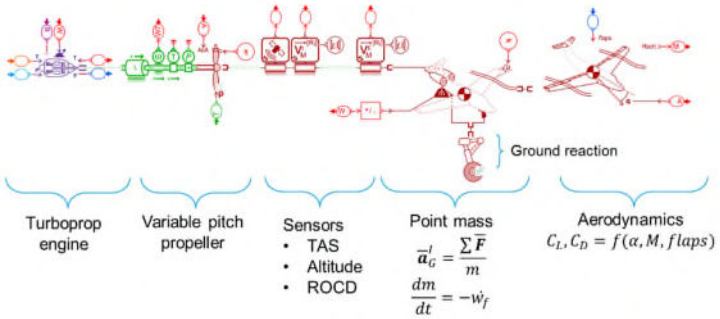

Figure 7: Simcenter Amesim aircraft performance model.

1. The aerodynamic efforts component, which computes lift and drag. The aerodynamic coefficients are provided by tables [26] and they depend on the angle of attack, the Mach number and of the flaps position.

2. The point mass component, that computes the acceleration, velocity and position of the aircraft center of mass depending on the forces applied, and the aircraft mass due to fuel consumption.

3. A set of sensors used to control the aircraft navigation.

4. The variable pitch propeller and the associated rotating inertia. This component computes the thrust generated by the propeller and the torque consumed. The ATR PW127 engines are equipped with Hamilton Sundstrand 568F propellers. The propeller characteristic is described by tables expressing the power and thrust coefficient as a function of the advance ratio and the blades pitch angle [26].
5. The leftmost component of ***Figure 7*** represents the PW127-M turboprop engine and it incapsulates the model shown in ***Figure 8***. According to the specifications [31], the engine comprises a three-spool turbomachine (including a free turbine), and a reduction gearbox. An LP centrifugal compressor, driven by a single stage LP turbine, boosts a centrifugal HP impeller, mounted on the same shaft as a single stage HP turbine. Power is delivered to the propeller through a gearbox via a third shaft, connected to a two-stage turbine. The power rating at maximum continuous thrust is 1840 kW. The model utilizes the Amesim readily available maps to define off-design performance for the turbomachinery components. Bleed off-take for the environmental control system, as well as the power required by the accessory gear box, are considered.

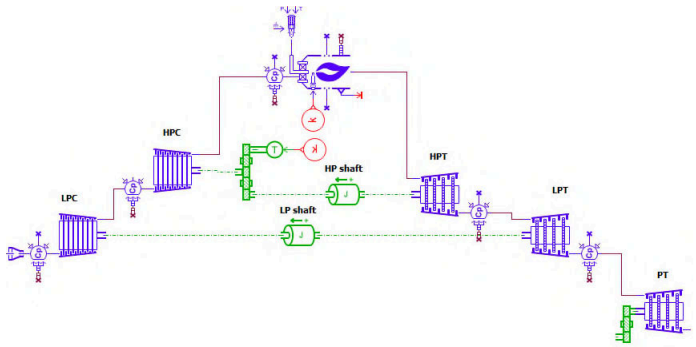

Figure 8: Simcenter Amesim gas turbine engine model.

The model validation was based on the data available in the FCOM [27]. For the climb phase, the FCOM provides the time, distance, fuel consumption, engine rotational speed and mean true airspeed of the aircraft for a given weight and flight level (altitude) to reach. For cruise, the data provided is the engine torque percentage, the fuel consumption, indicated and true airspeed. For descent, the data indicated is the same as for climb, with the difference that these are given for a determined indicated airspeed and flight path angle. With this information available, it was possible to generate a flight mission (altitude and speed versus time), provide it as a target to the aircraft performance model, and check if it is followed correctly, so as the fuel consumption.

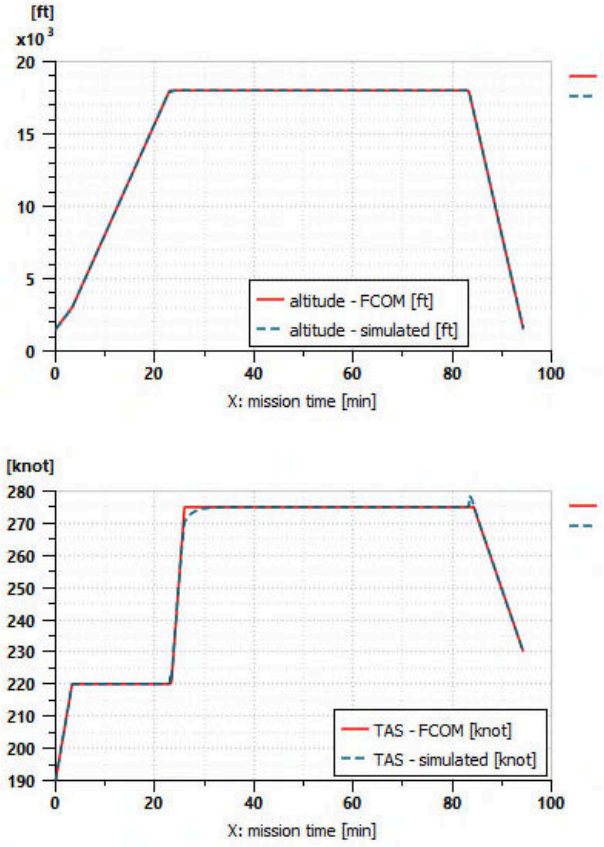

Figure 9: Plot of target and simulated flight mission of the ATR 72-600 model for a 400 nmi mission, TOW 22.5t.

Figure 9 shows the comparison of the altitude and speed profile described in the FCOM for a 400 nmi mission and the profile followed by the aircraft model. Minor differences are noticeable in the speed profile when switching from climb to cruise and cruise to descent, with a negligible impact on the performance analysis. ***Table 2*** summarizes the difference in the total flight time, fuel flow in cruise and total fuel burnt. As seen, there is good agreement between the model and the available data, hence the procedure followed can be considered suitable for developing a specific system model.

Table 2: Results validation of the ATR 72-600 model for a 400 nmi mission, TOW 22.5t.

	FCOM	Simulation	error
Flight time [min]	95.3	94.3	1.1%
Fuel flow cruise [kg/h]	620	620	0.1%
Total fuel burnt [kg]	1122	1120	-0.2%

A free-wake aerodynamics model coupled with an Acoustic-Analogy-based noise prediction tool [29] is employed for the prediction of rotor noise. The integrated method employs an unsteady aerodynamic representation of the rotor blades including the impact of tip vortices on the prediction of inflow, and an integral solution of the Ffowcs Williams-Hawkings equation for noise propagation [32]. The model is verified against wind tunnel data for the NASA SR-2 propeller, retrieved from [33]. The comparison in shown in ***Figure 10***. Overall Sound Pressure Level (OASPL) predictions are compared with microphone measurements taken at different angles from the propeller rotation axis. Overall, good agreement is observed between predicted and wind tunnel data, especially close to the direction of the rotor plane. Discrepancies of up to 17dB are calculated for measurement angles below 60 and above 120 deg., which is due to aerodynamic interactions and wind tunnel interference effects not captured by the model.

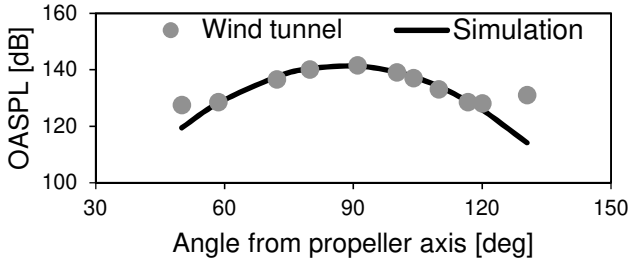

Figure 10: Overall Sound Pressure Levels (OASPL) prediction for NASA SR-2 propeller. Comparison with experimental data [33].

Having confirmed the validity of the noise prediction methodology, the tool is subsequently utilized in the prediction of ATR-42-500 aircraft propellers during take-off. Reconstruction of HS-568-F propeller geometry was conducted for the specific geometry, and where data was unavailable, literature suggestions where used [34]. In addition, the airfoils along the span of the propeller blade were represented by NACA 16-series profile, with experimental data from [35]. The parameters which govern propeller noise generation are: (a) rotational speed which primarily affects in-plane thickness and high-speed impulsive noise and (b) thrust requirements, which affect both in-plane and out-of-plane loading noise. It is noted that the employed method is not capable of predicting high-speed impulsive noise generated by transonic flow near the tip of high-speed propellers; however, it can quantify the primary effects of rotor speed and thrust variation on ground noise emissions.

ATR 42-500 modeling and validation

Having validated the modeling strategy with the ATR 72-600 performance model, the performance model of the ATR 42-500 was obtained down-scaling the engine to provide a maximum continuous shaft power of 1790 kW and modifying the aerodynamics coefficient to account for the different geometry. The first task is quickly accomplished thanks to the map scaling tool associated to the compressor and turbine components of Amesim's gas turbine library [36]. The aerodynamics coefficient correction for the shorter fuselage was performed using the methods provided in [37]. The ATR 42-500 performance model was validated in the same way as the ATR 72-600. The target and the simulated mission profiles are plotted in ***Figure 11.***

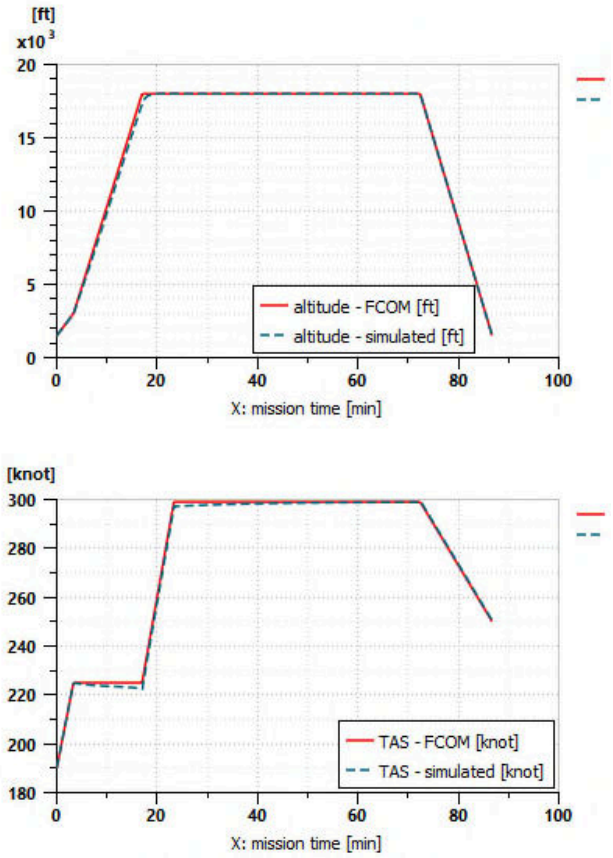

Figure 11: Plot of target and simulated flight mission of the ATR 42-500 model for a 400 nmi mission, TOW 18.5t.

***Table* 3** shows the differences of total flight time, fuel flow in cruise and total fuel burnt. The validation was deemed successful.

Table 3: results validation of the ATR 42-500 model for a 400 nmi mission, TOW 18.5t.

	FCOM	Simulation	error
Flight time [min]	88.4	86.8	-1.8%
Fuel flow cruise [kg/h]	786	788	-0.2%
Fuel burnt [kg]	1110	1120	0.9%

.

ATR 42-500 parallel hybrid variants

The next step of the study consisted in modeling the hybridized version of the ATR42-500. This was achieved coupling the gas turbine to an electric motor through a gearbox driving the propeller, as shown in ***Figure 12*****,** according to the parallel configuration presented in ***Figure 5*****.**

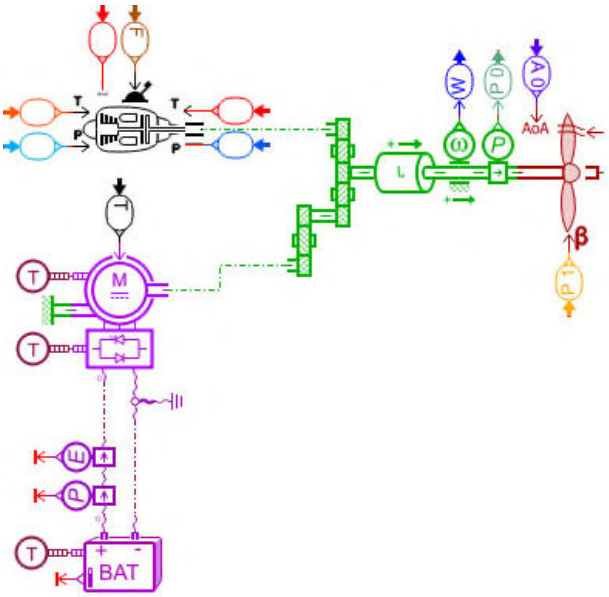

Figure 12: Simcenter Amesim aircraft performance model. Focus on the hybrid-propulsion powerplant.

The nominal installed propulsive power of the hybrid versions was modeled to be equal to the conventional aircraft. As in the conventional ATR the maximum continuous power rating per engine is $P_{MCT} = 1790\ kW$, the same rating was used to size the coupling of the electric motor and the gas turbine. The relation between the two systems power is defined by hybridization degree (H_p). For increasing the hybridization, the engine is scaled down assuming the same cycle in terms of specific power and scaling the turbomachinery components design inlet mass flow accordingly.

The scaling down process has also the side effect to slightly decrease the turbomachine weight. Correlation of corrected mass flow versus weight was used to account for this effect in the determination of the aircraft OEW [38].

The electric motor was sized to provide a power rating equal to $P_{MCT} \cdot H_P$. The component chosen to represent its behavior is a quasi-static model of an electric drive system consisting of a machine, an inverter, and control unit. This component assumes the motor and the inverter efficiency to be constant, so as the maximum power, maximum torque, and maximum speed. This assumption was imposed by the lack of data necessary for higher fidelity motors, which require to provide information on how the parameters vary with respect to the operating conditions. The power density of the electric motor was assumed to be 5.2 kW/kg, in-line with the current state-of-the-art Siemens sp260d [39]. Considered the projection of the evolution in electric motors power density [40], this is a conservative assumption for an entry into service planned for 2030.

Due to its low energy density with respect to fuel, batteries represent a significant portion of the aircraft TOW. These were sized to provide the energy necessary for the nominal mission, as the second part of the "reserve" mission is completed relying just on the gas turbine. An additional hypothesis consisted in limiting the depth of discharge to 80%, following a rule of thumb aiming at preserving the battery's lifetime.

In the Amesim component, the battery's cells are modeled as an equivalent circuit with a resistor and a capacitance in series. The desired nominal capacitance and the open circuit voltage are achieved adding cells in parallel and series respectively. Assuming that in 2030 cell's capacity will follow the same trend as the specific energy density, a value of 400 Ah was considered. The electrical system nominal voltage is set to 540V. Based on the performance of lithium-manganese-cobalt-oxide batteries, the cells nominal voltage selected was 3.7 V [41] . The sizing details of battery packs for the configurations assessed are detailed in ***Table 4***.

Table 4: Battery pack details.

Hp	Target power	Target voltage	Target energy	Nominal capacity	# cell series	# cell parallel
%	kW	V	kWh	Ah	-	-
20	358	540	405	750	148	2
40	716	540	891	1650	148	4
60	1074	540	1387	2568	148	6

Figure *13* shows the C rate curves obtained with the Simcenter Amesim dedicated module that represents the performance need from the batteries to obtain the targets set above. In the missions simulated, the C rate is included between 0.5 and 1, and it is therefore deemed as acceptable. In addition, the state of charge is limited at 20%, as required. The dependence of voltage and resistance (losses) with respect to the temperature was neglected in this study.

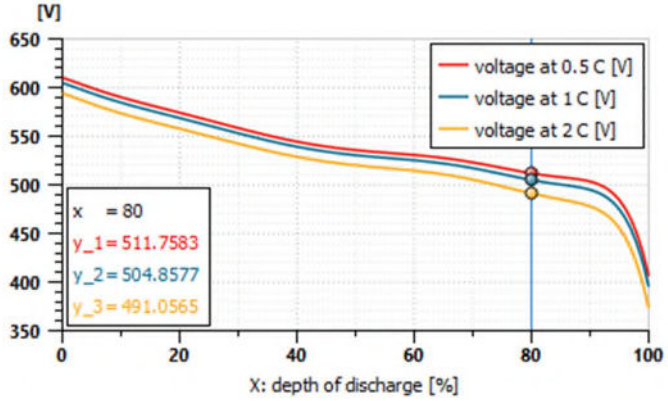

Figure 13: Batteries C rate curves.

The addition of a second source of energy for the propulsion provides significant flexibility on energy management strategies. For instance, it is possible to utilize electrical energy only during climb, so that the gas turbine works closer to its optimum design point (usually cruise) during the whole flight. Another option would be recharging batteries during descent. Additionally, gas turbines could be completely switched off during descent and approach, relying only on the electric propulsion for these low energy flight segments, with improvements in noise and pollutant emissions as the aircraft gets closer to the ground, albeit aspects of safety and redundancy should be assessed. For this analysis, it was chosen to select the energy management strategy that allows to minimize aircraft weight and maximize ESAR. For this reason, the batteries are sized to provide energy just during climb and cruise, with the electric motor switched off during descent. The power split for the cases assessed herein is depicted in ***Figure 14***.

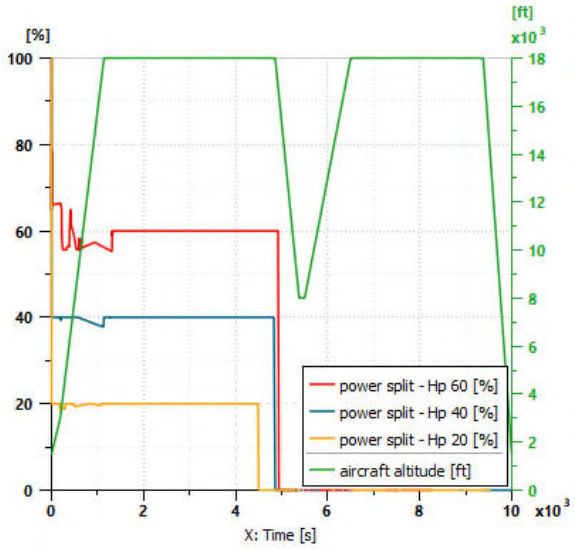

Figure 14: Fraction of power provided by the electric motors versus the overall propulsive power.

The TOW of the three hybrid versions, displayed in **Figure *15***, were obtained as follows:

- The payload is 5300 kg, as per requirements (48 pax).
- The OEW comprises the weight of the structure, the systems, and the engines. It was obtained adjusting the conventional aircraft OEW considering the rescaled gas turbines and electric motors. The weight reduction of the former almost compensate the increase of the latter, providing a very similar OEW across the versions compared.
- The weight of the mission fuel (used for the nominal part of the mission), the reserve fuel (burnt to reach the alternate airport and ensure additional 45 minutes flight) and the batteries were determined iteratively.

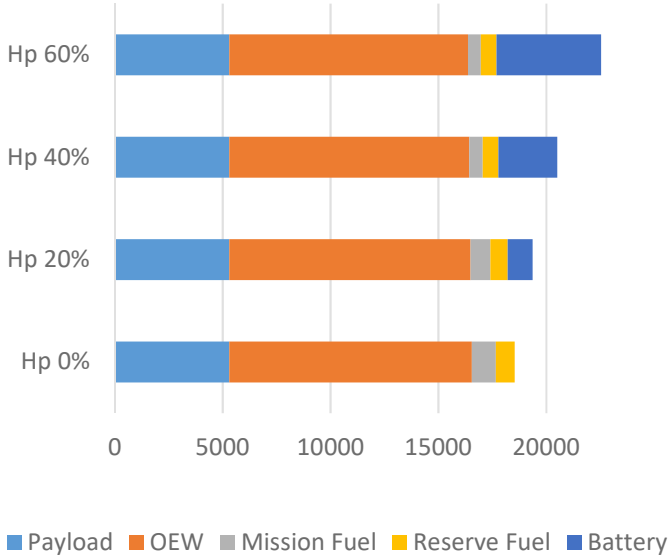

Figure 15: Breakdown weight comparison for different hybridization degrees for a "reserve" mission. Weights in kg.

It should be highlighted that the MTOW weight of the conventional ATR 42-500 is 18600 kg, which is exceeded by the hybrid versions. To cope with that, it was decided to use a slightly higher L/D ratio than the one obtained from the drag polar of [25] and [26]. This follows the approach proposed in [10], and it reflects the improvement in aerodynamics that can be achieved by 2030. The enhanced L/D ratio selected for the study is to 15 at the start of cruise, where the initial value is

12. To provide a fair comparison, the same aerodynamic performance was used for the three hybrid and the conventional version.

Table 5 below summarizes the TOW and the ESAR obtained in cruise for the configurations evaluated. The 40% variant is the one that obtains the highest ESAR. For the 60% degree of hybridization, the weight penalty of the batteries has an impact on the overall aircraft efficiency.

Table 5: Summary TOW, ESAR at cruise and its percentuale increase with respect to the baseline for the configurations evaluated.

HP		**0%**	**20%**	**40%**	**60%**
TOW	tons	18,60	19,37	20,52	22,55
ESAR cruise	m/MJ	**16,70**	**18,79**	**24,63**	**23,28**
ΔESAR	%	**-**	**12,51**	**47,49**	**39,40**

While the 20% hybrid version could follow the mission profile prescribed in the FCOM, the 40% showed a degraded performance, nevertheless acceptable, in the second part of the reserve mission (***Figure 16***). The rate of climb of the aircraft is lower than what found in the FCOM. The results of 60% hybrid version are depicted in ***Figure 17***. It is evident how the de-rated gas turbines do not provide adequate power for completing the reserve mission. The aircraft altitude and speed decreases from the instant that the electric motors are switched off. This configuration does not allow to complete the reserve mission scenario, as required for this study.

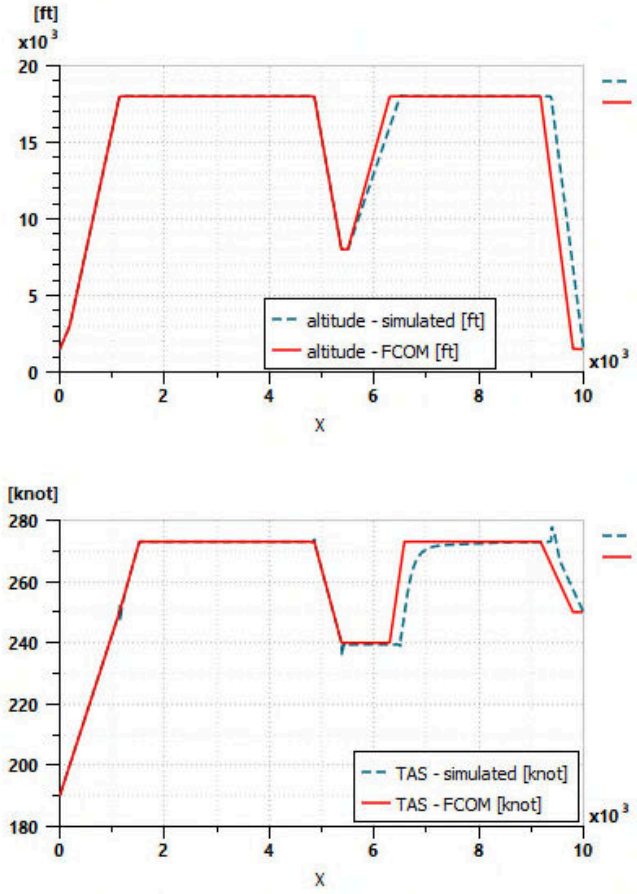

Figure 16: Plot of target and simulated flight mission of the 40% hybrid version of the ATR 42-500 model for a "reserve" mission, TOW 20.5t.

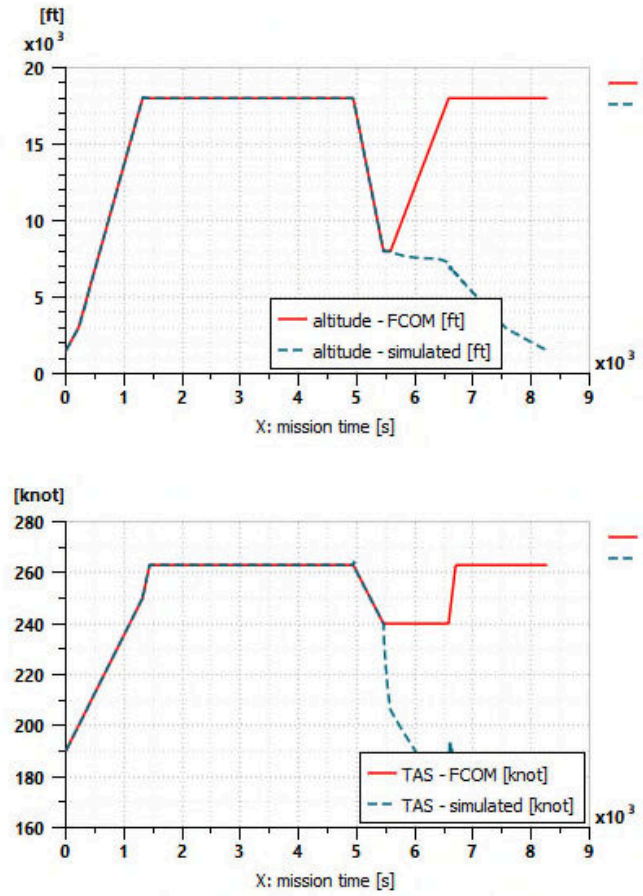

Figure 17: Plot of target and simulated flight mission of the 60% hybrid version of the ATR 42-500 model for a "reserve" mission, TOW 22.5t.

Pollutant emissions and acoustics analysis

The NO_x, CO_2 and H_2O emissions computed for the nominal mission of the three hybrid degrees variants are compared with respect to the baseline and presented in ***Figure 18***.

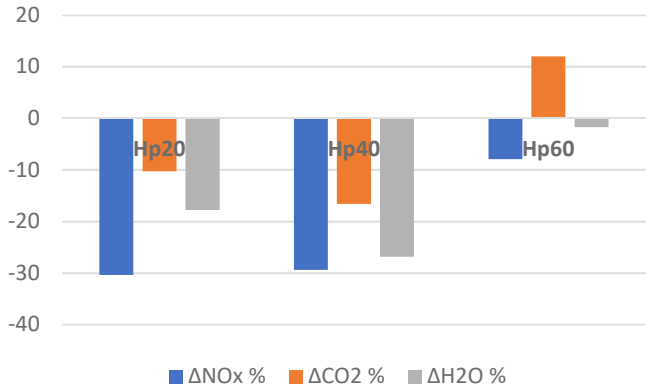

Figure 18: Emissions comparison for different hybridization degrees with respect to the baseline for a nominal mission.

As expected, NO_x and H_2O emissions decrease proportionally with the fuel consumed. However, as CO_2 emissions also accounts for the battery energy consumption, one can notice that the 40% hybrid variant releases less carbon dioxide than the 60%. This is consistent with the findings on the ESAR discussed above, according to which the 40% hybrid version is

more energy efficient, hence less polluting, than the 60%. Comparing the 40% hybrid variant with the conventional baseline, the reduction in CO_2 and NO_x emissions are of 27% and 60% respectively. These results are still far from the ACARE targets for 2050 of 75% and 90%. However, considering that the simulation results were computed accounting for a technologies levels assumed available for an entry into service in 2035, they look promising.

Figure 19 (a) presents the employed rotor speed schedules and ***Figure 19 (b)*** the associated two rotors thrust requirements during take-off for different levels of hybridization.

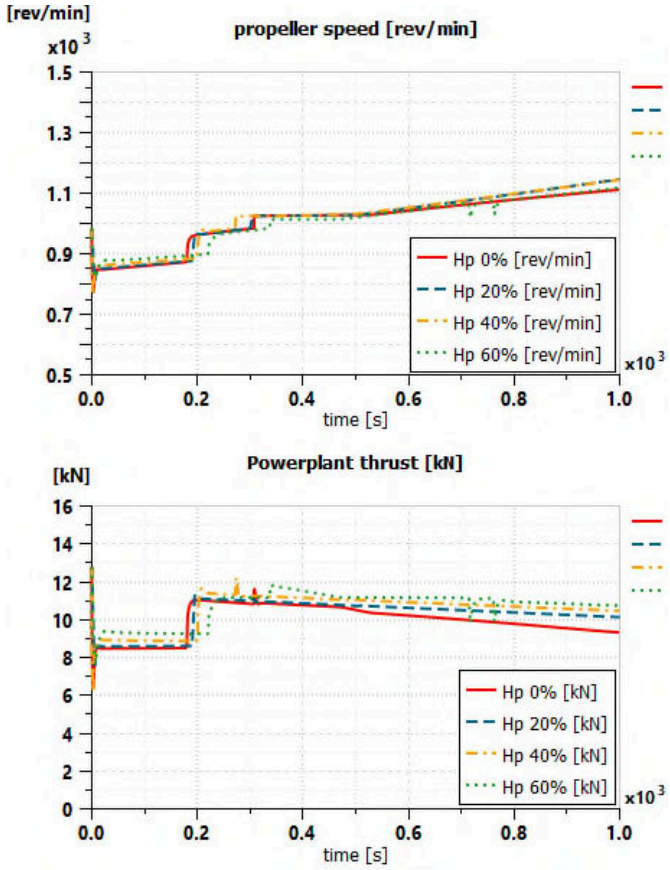

Figure 19: Variation of rotor speed settings and thrust requirements during take-off.

Figure 20 (a) illustrates the corresponding noise footprint for Hp=0%. Noise deltas are calculated for the Sound Exposure Levels (SEL) of Hp=20%, Hp=40% and Hp=60% with respect to the Hp=0% case, as shown in ***Figure 20 (b)-(d).*** It is noted that negative deltas represent noise reductions. The increase in MTOW is reflected on the rotor speed and thrust requirements in climb. Consequently, the corresponding SEL deltas are between 0.5-1 dB for Hp=20%, 1-2 dB for Hp=40% and 2-3 dB for Hp=60%. Therefore, the powerplant performance benefits accrued from hybridization are compromised by an increase in the associated ground noise impact.

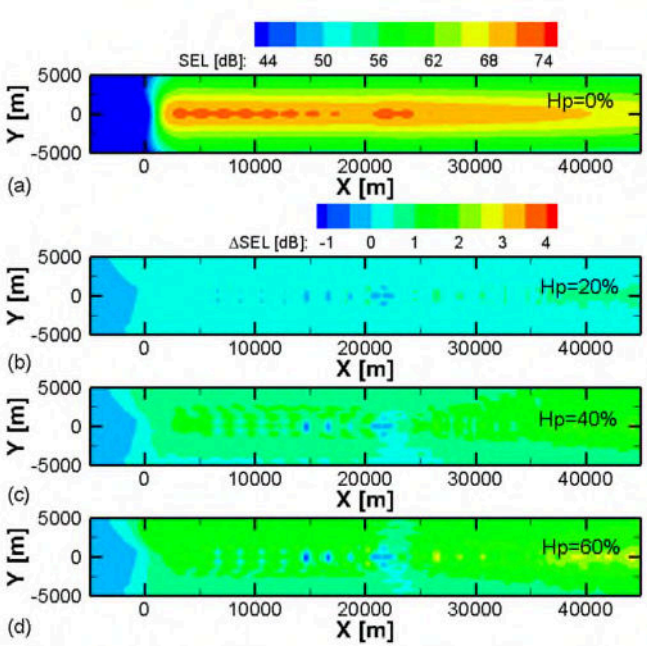

Figure 20: Sound Exposure Levels (SEL) and associated deltas in climb for different levels of hybridization: (a) Hp=0%; (b) Hp=20%; (c) Hp=40%; (d) Hp=60%.

CONCLUSION

The MBSE ARCADIA methodology was successfully applied to develop operational, system, logical and simulation architecture of a hybrid aircraft use-case. Starting from top level aircraft requirements, the operational architecture was built which was continuously refined and elaborated to obtain the logical architecture. Using the methodology proposed in the project, a successful transition to system simulation was performed. The behavioral models in Amesim then allowed simulating the aircraft in multiple mission scenarios to answer the different questions raised by architecture models regarding the degree of hybridization, weight of the aircraft, etc. Validated models of ATR 42 and ATR 72 were obtained in Amesim. Three hybrid models with different degree of hybridization were developed according to the specifications from system architecture models.

The simulations performed on the baseline and hybrid models in Amesim provided a way to analyze the performance of the models. As expected, the weight of the models increased with hybridization due to the strong influence of batteries. The analysis showed that ESAR increases with hybridization up to a certain point after which it reduces due to the high weight of batteries. Hybridization level of 40% was found to be the best variant among the assessed hybrid models. However, in terms of noise, it was shown that the powerplant performance benefits accrued from hybridization are compromised by an increase in the associated ground noise impact.

The results yielded from simulation can be utilized to freeze the logical architecture and advance to further stages of architecture like physical analysis. With the proposed methodology, the simulation results are embedded to the model which will allow further refinement and iterations of sub-systems. This project showcased the potential of using system architecting and system simulation activities in synergy. This can facilitate the deployment of MBSE, with the consequent benefits of improved design quality, improved communication between design stakeholders, decrease of errors found late stages, and finally time and cost savings in the design process [5].

ACKNOWLEDGEMENTS

The author would like to thank Mr. Sagar Shenoy Manikar for his contribution to this paper during his internship at Siemens Digital Industries Software.

REFERENCES

[1] Remy, S. "Innovation in Aircraft complex systems integration". ICAS Workshop 2015 on Complex Systems Integration in Aeronautics.

[2] Ying, S. X. "Report from ICAS Workshop on Complex Systems Integration in Aeronautics". 30th Congress of the International Council of Aeronautical Sciences, 2016.

[3] Crawley, E.; Cameron, B. and Selva, D. 2015. "System Architecture: Strategy and Product Development for Complex Systems (1st. ed.)". Prentice Hall Press, USA.

[4] CESAM: CESAMES systems architecting method. A pocket guide, 2017, [online] Available: http://www.cesames.net/wp-content/uploads/2017/05/CESAM-guide.pdf.

[5] Hart, L. E. "Introduction to Model-Based System Engineering (MBSE) and SysML". Delaware Valley INCOSE Chapter Meeting, 2015.

[6] Haskins, B.; Stecklein, J.; Dick, B.; Moroney, G.; Lovell, R. and Dabney, J. (2004). 8.4.2 "Error Cost Escalation Through the Project Life Cycle". INCOSE International Symposium. 14. 1723-1737. 10.1002/j.2334-5837.2004.tb00608.x.

[7] Cappuzzo, F.; Broca, O. and Allain, L. "Methodologies and processes to achieve earlier virtual integration of aircraft systems", 6th European Conference for Aerospace Sciences, 2015.

[8] Airbus' Global Market Forecast. https://www.airbus.com/aircraft/market/global-market-forecast.html

[9] Flightpath 2050 Goals, Advisory Council for Aviation research and innovation in Europe (ACARE), https://www.acare4europe.org/sria/flightpath-2050-goals/protecting-environment-and-energy-supply-0

[10] Antcliff, K.R. et al. "Mission Analysis and Aircraft Sizing of a Hybrid-Electric Regional Aircraft". 54th AIAA Aerospace Sciences Meeting. San Diego, California, USA. 4-8 January 2016. https://doi.org/10.2514/6.2016-1028

[11] Antcliff, K. R. and Capristan, F. M. "Conceptual Design of the Parallel Electric-Gas Architecture with Synergistic Utilization Scheme (PEGASUS) Concept". 18th AIAA/ISSMO Multidisciplinary Analysis and Optimization Conference, Denver, CO, 2017. https://doi.org/10.2514/6.2017-4001

[12] Marien, T. "Seat Capacity Selection for an Advanced Short-Haul Aircraft Design", 54th AIAA Aerospace Sciences Meeting, AIAA SciTech, American Institute of Aeronautics and Astronautics, January 2016, https://doi.org/10.2514/6.2016-1283

[13] Wikipedia, List of regional airliners. https://en.wikipedia.org/wiki/List_of_regional_airliners

[14] EASA - Annexes to the draft Commission Regulation on 'Air Operations - OPS' https://www.easa.europa.eu/sites/default/files/dfu/Annexes%20to%20Regulation.pdf CAT.OP.MPA.151 Fuel policy — alleviations

[15] ATR DC/E Marketing September 2014, http://www.atraircraft.com/datas/download_center/34/fiches_500_septembre2014_34.pdf, (accessed July 2019)

[16] Brelje, B. J. and Martins, J. R. R. A. "Electric, Hybrid, and Turboelectric Fixed-Wing Aircraft: A Review of Concepts, Models, and Design Approaches", Progress in Aerospace Sciences, 2018. doi:10.1016/j.paerosci.2018.06.004

[17] Kuhn, H., Sizmann, A., "Fundamental Prerequisites for Electric Flying", 61. Deutscher Luft- und Raumfahrt-Kongress (DLRK), Berlin, Germany, 10-12 September, 2012

[18] Wu, J. "Challenge and Opportunity of Advanced Materials and Chemistries for Electrochemical Energy Storages Development of NASA Future Missions", Seminar at Department of Chemistry and Biochemistry, University of California at Santa Cruz, California, April 2, 2018 https://ntrs.nasa.gov/archive/nasa/casi.ntrs.nasa.gov/20180004547.pdf (accessed Sept 2019)

[19] Isikveren, A.T.; Kaiser, S.; Pornet, S. C. and Vratny, P.C. "Pre-design strategies and sizing techniques for dual-energy aircraft". Aircraft Engineering and Aerospace Technology: An International Journal. Volume 86 · Number 6 · 2014 · 525–542. DOI 10.1108/AEAT-08-2014-0122

[20] Rindlisbacher, T. "Guidance on the Determination of Helicopter Emissions". Swiss Confederation Federal Office of Civil Aviation (FOCA), Ref. 0/3/33/33D05D20, Bern, Switzerland, March, 2009.

[21] International Energy Agency (IEA). Recent Trends in the OECD: Energy and CO2 Emissions; International Energy Agency (IEA): Paris, France, 2016.

[22] Architecture Analysis and Design Integrated Approach (ARCADIA) Method https://www.polarsys.org/capella/arcadia.html

[23] Roques, P. "MBSE with the ARCADIA Method and the Capella Tool". 8th European Congress on Embedded Real Time Software and Systems (ERTS 2016), Jan 2016, Toulouse, France. ffhal-01258014

[24] Siemens Digital Industries Software. Simcenter Amesim, https://www.plm.automation.siemens.com/global/en/products/simcenter/simcenter-amesim.html

[25] Niță M.F. "Aircraft Design Studies Based on the ATR 72", June 2018, Hamburg university of applied sciences.

[26] Filippone, A. "Advanced Aircraft Flight Performance", 2012, Cambridge University Press, ISBN 978-1-107-02400-7

[27] ATR 72 Flight Crew Operating Manual (FCOM)

[28] ATR 42 Flight Crew Operating Manual (FCOM)

[29] Vouros, S.; Goulos, I. and Pachidis, V. "Integrated methodology for the prediction of helicopter rotor noise at mission level," Aerosp. Sci. Technol., vol. 89, pp. 136–149, 2019.

[30] Zipfel, P.; "Modeling and Simulation of Aerospace Vehicle Dynamics", 2006, 2nd Edition, Reston: American Institute of Aeronautics and Astronautics.

[31] "Type certificate data sheet for PW100 series engines". EASA. 80 March 2018. https://www.easa.europa.eu/sites/default/files/dfu/EASA%20IM.E.041%20TCDS%20Issue%204.pdf

[32] Brentner, K. S.; Farassat, F. (2003). "Modeling aerodynamically generated sound of helicopter rotors". *Progress in Aerospace Sciences*, *39*(2-3), 83-120.

[33] Dittmar, J. H. (1989). "Cruise noise of the SR-2 propeller model in a wind tunnel", NASA/TM 101480.

[34] Filippone, A., and Mohamed-Kassim, Z., "Multi-Disciplinary Simulation of Propeller-Turboprop Aircraft Flight," Aeronautical Journal, Vol.116 No.1184, (2012), pp. 985–1014, DOI 10.1017/S0001924000007454.

[35] Lord, B. N. D. and D. R., "Aerodynamic Characteristics of Several 6% Thick Airfoil at Angle of Attack from 0^0 to 20^0 at High Subsonic Speed", *NACA TECHNICAL NOTE 3424* (1955).

[36] Roumeliotis, I.; Mourouzidis, C.; Zafferetti, M.; Pachidis, V.; Broca, O. and Unlu, D. "Assessment of Thermo-Electric Power Plants for Rotorcraft Application". Proceedings of ASME Turbo Expo 2019: Turbomachinery Technical Conference and Exposition. June 17-21, 2019, Phoenix, Arizona, USA.

[37] Roskam, J. (1997). Airplane design. Lawrence, Kan: DARcorporation.

[38] Lolis, P., (2014), "Development of a Novel Preliminary Aero Engine Weight Estimation Method", PhD Thesis, Propulsion Engineering Centre, Cranfield University, 2014

[39] Wikipedia, https://en.wikipedia.org/wiki/Siemens_SP260D

[40] Clarke, S. "Aircraft Electric Propulsion Systems: Applied Research at NASA". 2015 IEEE Transportation Electrification Conference and Expo, Dearborn, Michigan, June 17, 2015.

[41] Miao, Y.; Hynan, P.; von Jouanne, A.; Yokochi, A. "Current Li-Ion Battery Technologies in Electric Vehicles and Opportunities for Advancements". Energies 2019, 12, 1074.

[42] International Energy Agency (IEA). Recent Trends in the OECD: Energy and CO2 Emissions; International Energy Agency (IEA): Paris, France, 2016

[43] Rindlisbacher, T. (2009). "Guidance on the determination of helicopter emissions". Federal Office of Civil Aviation (FOCA), Division Aviation Policy and Strategy, Bern, Switzerland, Reference No. 0/3/2033/33-05-20